2011

Treatment of saline aqueous solutions using direct contact membrane distillation

Long Nghiem
University of Wollongong, longn@uow.edu.au

Florian Hildinger
University of Wollongong

Faisal I. Hai
University of Wollongong, faisal@uow.edu.au

Tzahi Cath
Colorado School Of Mines

Publication Details

Nghiem, L. D., Hildinger, F., Hai, F. I. & Cath, T. (2011). Treatment of saline aqueous solutions using direct contact membrane distillation. Desalination and Water Treatment, 32 234-241.

TREATMENT OF SALINE AQUEOUS SOLUTIONS USING DIRECT CONTACT MEMBRANE DISTILLATION

Long D. Nghiem[1,], Florian Hildinger[1], Faisal I. Hai[1], Tzahi Cath[2]*

[1] School of Civil, Mining and Environmental Engineering
The University of Wollongong, Wollongong, NSW 2522, Australia

[2] Division of Environmental Science and Engineering
Colorado School of Mines, Golden, CO, 80401 USA

** Corresponding author: longn@uow.edu.au*

ABSTRACT: The treatment of highly saline aqueous solutions using direct contact membrane distillation (DCMD) was evaluated in this study. Experiments were conducted using a flat sheet polytetrafluoroethylene membrane with nominal pore size of 0.22 μm. Seawater, reverse osmosis (RO) concentrate collected from a wastewater reclamation plant, and a synthetic solution containing 2,000 mg/L of $CaSO_4$ were selected as the representative saline solutions. A gradual decline in permeate flux was observed at the beginning of the experiments when the seawater and RO concentrate solutions were treated using the DCMD process, most likely due to initial organic fouling and scaling. In contrast, when the saturated $CaSO_4$ solution was used as the feed, the permeate flux was stable for approximately 300 minutes of operation. However, when these solutions were concentrated beyond their solubility limit, crystallization of the sparingly soluble salts occurred on the membrane surface, leading to a complete loss of permeate flux at the end of the experiment. Contact angle measurement of the fouled and scaled membranes revealed a significant reduction in hydrophobicity. Membrane fouling and scaling were also confirmed by scanning electron microscopy analysis. The results suggest that pretreatment to remove organic matter is essential to prevent organic fouling. In addition, a major limiting factor for the treatment of saline solutions using DCMD appears to be the solubility of sparingly soluble salts.

Keywords: Direct contact membrane distillation (DCMD), organic fouling, RO concentrate, scaling, saline solution.

1. Introduction

Membrane distillation (MD) is a thermally driven desalination process that involves phase conversion from liquid to vapor on one side of the membrane and condensation of vapor to liquid on the other side [1]. The membrane facilitates the transport of water vapor through its pores but does not participate in the actual separation process. Although the process of MD is not new, it has only recently been recognized as a low cost, energy saving alternative to conventional separation processes for the treatment of saline water and wastewater such as thermal distillation and reverse osmosis [2-3]. MD has several advantages compared to conventional thermal distillation and reverse osmosis processes [3-4]. Because water is transported through the membrane only in a vapor phase, MD can offer complete rejection of all non-volatile constituents in the feed solution; thus, almost 100% rejection of ions, dissolved non-volatile organics, colloids, and pathogenic agents can be achieved via the MD process. More importantly, due to the discontinuity of the liquid phase across the membrane, the mass flux in an MD process is not subjected to an osmotic pressure gradient. Consequently, the greatest potential of MD can be realized for the treatment of highly saline solutions [5]. In fact, it has been experimentally demonstrated that the permeate flux of an MD process is independent of the feed water salinity up to 76,000 mg/L total dissolved solids (TDS), which is twice the salinity of a typical seawater [6]. MD also requires lower operating pressures than reverse osmosis membrane separation processes. In a typical MD process, since the applied pressure is negligible and the feed solution does not enter the membrane pores, chemical interactions between membrane and process solutions are less intense [1]. In addition, MD requires lower operating temperatures than conventional distillation, which can facilitate the utilization of low grade heat [1, 7]. The unique ability of MD to utilize low grade heat from industrial sources (which may otherwise be wasted) or solar thermal energy provides an excellent platform for a greenhouse neutral desalination process [1].

The driving force of the process is supplied by the vapor pressure difference induced by temperature difference between the liquid–vapor interfaces on the feed and distillate sides of the membrane. MD can be employed in several different configurations [1]. Among them, the direct contact membrane distillation (DCMD) configuration is best suited for applications such as desalination or the concentration of aqueous solutions, in which water is the major permeate component [8-9]. Indeed, DCMD requires the least equipment and is the simplest to operate [8]. MD has potential applications in many areas of scientific and industrial interest, yielding highly purified permeate and separating contaminants from liquid solutions. It has been tested for the treatment of thermally sensitive industrial products such as concentrating aqueous solution in fruit juices, the biotechnology industry, as well as for wastewater treatment and water desalination [5, 10-18]. Since the process of membrane distillation is independent of the solution osmotic pressure (or salinity), MD is particularly ideal for the treatment of saline solution such as RO concentrate from inland water recycling or brackish water desalination applications [4-5, 19].

While MD has been extensively studied over the last few years, it is noteworthy that the process of membrane scaling and fouling has not yet been adequately investigated [16, 20]. Recent studies have revealed that the scaling phenomenon observed in MD can remarkably differ from that of a typical pressure driven membrane filtration process. For example, while $CaCO_3$ has been known to be a very potent scalant during a typical nanofiltration or reverse osmosis process, it was not the case during membrane distillation [21]. In contrast, membrane scaling in DCMD due to the precipitation of gypsum ($CaSO_4$) could be severe, leading to a dramatic flux decline [21]. These salient aspects are in fact very important if MD will be used for the treatment of highly saline wastewater containing sparingly soluble salts. Accordingly, the objective of this study was to assess the membrane fouling and scaling phenomena during the treatment of highly saline aqueous solutions using DCMD.

2. Materials and Methods

2.1. DCMD test unit and experimental procedure

DCMD experiments were conducted using a closed-loop bench-scale membrane test unit (Figure 1). The membrane cell was made of acrylic plastic to minimize heat loss to the surroundings. It was designed to hold a flat-sheet membrane under moderate pressure gradients without any physical support. The flow channels were engraved in each of two acrylic blocks that made up the feed and permeate semi-cells. Each channel was 0.3 cm deep, 9.5 cm wide, and 14.5 cm long; and the total active membrane area for mass transfer was 138 cm^2.

Feed solution was circulated from a stainless steel feed reservoir through the feed membrane semi-cell and back to the reservoir. A heating element encased inside a stainless steel tube was placed directly into the feed reservoir. A temperature sensor was placed immediately before the inlet of the feed solution to the membrane cell. The heating element and the temperature sensor were connected to a temperature control unit to regulate the temperature of the feed solution. MilliQ water was used as the initial condensing fluid. The distillate was circulated from a 2 L Perspex reservoir through the distillate membrane semi-cell and back to the reservoir. The distillate reservoir allowed overflow of excess permeating water into a collecting container. The overflowing distillate was continuously weighed on an electronic balance (PB32002-S, Mettler Toledo Inc., Hightstown, NJ). Another temperature sensor was installed immediately at the outlet of the distillate semi-cell. The temperature of the distillate was regulated using two cooling units (Neslab RTE 7, Thermo Fisher Scientific, Waltham, MA, USA) equipped with a stainless steel heat-exchanging coil, which was submerged in the distillate reservoir. Two pumps (Model 120/IEC71-B14, Micropump Inc., Vancouver, WA, USA) were used to circulate feed and distillate from their respective reservoirs through the membrane cell and back to the reservoirs (at up to 4 L/min and 70 °C). Flow rates of the feed

and distillate were monitored using two rotameters and were kept constant and similar at all times. All the pipes used in the DCMD test unit were covered with insulation foam to minimise heat loss.

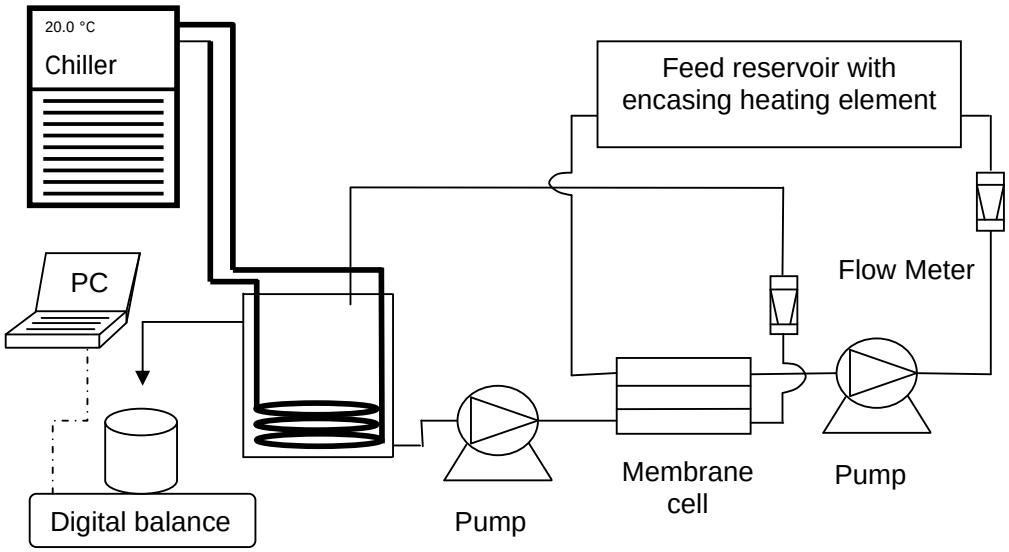

Figure 1: Schematic diagram of the CDMD system.

A feed volume of 10 L was used in all experiments in this study. Temperature of the distillate was kept constant at 20 °C. When evaluating the performance of the DCMD system using tap water, permeate flux was measured for at least 2 hours at each feed temperature. A new membrane sample was used for each experiment in this study. At the completion of each experiment, the membrane was removed from the cell, air dried, and kept in a desiccator until surface analysis.

2.2. Microporous membrane

A hydrophobic, microporous membranes were acquired from (GE Osmonics, Minnetonka, MN) for this investigation. This is a composite membrane having a thin polytetrafluoroethylene (PTFE) active layer on top of a polypropylene (PP) support sublayer. The pore size and porosity of the membrane are 0.22 μm and 70%, respectively. The membrane thickness is 175 μm, of which the active layer is 5-10 μm.

2.3. Chemical reagents and test solutions

Three different saline solutions were used in this investigation. An RO concentrate solution was obtained from the Wollongong Water Recycling plant (Wollongong, Australia). Seawater was obtained from Wollongong beach which opens out to the Tasman Sea. Both the RO concentrate solution and seawater were used directly in the DCMD without any pretreatment. Analytical grade $CaSO_4$ obtained from Sigma-Aldrich (Castle Hill, Australia) was dissolved into MilliQ water to make up a saturated solution (2,000 mg/L) of $CaSO_4$. The compositions of the three test solutions are presented in Table 1. These three solutions represent three different scenarios involving the treatment of saline solution. The RO concentrate solution has a relatively low salinity with TDS of just over 4,000 mg/L but has significant organic matter content (Table 1). In contrast, the presence of organic matter in both the seawater and the synthetic $CaSO_4$ solution used in this study was negligible. Although TDS concentration of the synthetic gypsum solution is relatively low, the solution was at saturation with respect to $CaSO_4$.

Table 1: Characteristics of the test solutions used in this study.

Parameter	RO Concentrate	Seawater	Synthetic solution
pH (-)	8.1	8.2 – 8.66	6.0
Total Organic Carbon (mg/L)	33	<3	<1
Total Alkalinity as $CaCO_3$ (mg/L)	690	117 – 129	<10
Electrical Conductivity (mS/cm)	6.7	43.6 – 49.0	2.5
Calcium (mg/L)	150	350 – 510	588
Magnesium (mg/L)	140	1,100 – 1,500	
Sodium (mg/L)	1,200	9,920 – 12,000	
Potassium (mg/L)	97	350 – 600	
Silicon (mg/L)	26	0.1 – 0.3	
Bicarbonate (mg/L)	580	106 – 132	
Chloride (mg/L)	1,800	18,000 – 22,000	
Sulfate (mg/L)	380	2,300 – 3,584	1,412
Total dissolved solid (mg/L)	4,347	32,903 – 39,272	2,000

2.4. Analytical techniques

Conductivity and pH were measured using an Orion 4-Star Plus pH/conductivity meter (Thermo Fisher Scientific, Waltham, MA, USA). The conductivity probe was immerged directly into the permeate container to allow for continuous monitoring of the permeate

conductivity. The morphology and the composition of the fouling layer deposited onto the membrane surface were examined by scanning electron microscopy (SEM) using a JEOL JSM-6460A instrument (Tokyo, Japan), with additional semi-quantitative energy dispersive spectrometer (EDS) analysis. Prior to SEM analysis, the membrane samples were air-dried and subsequently coated with an ultrathin layer of carbon. Extreme care was taken when preparing the fouled and scaled membrane samples to ensure that the fouling and scaling layer remained intact. Contact angle measurements of the membrane surfaces were performed with a Rame-Hart Goniometer (Model 250, Rame-Hart, Netcong, NJ) using the standard sessile drop method. Milli-Q water was used as the reference solvent. The membrane samples were air dried prior to the measurement. At least 5 droplets were applied onto duplicate membrane samples.

3. Results and Discussion

3.1. DCMD of a diluted solution

The driving force in DCMD is a vapor pressure difference across the membrane, which is usually induced by a temperature difference between the feed and distillate sides of the membrane. In general, it can be assumed that the kinetic effects at the vapor-liquid interface are negligible. This assumption is valid at steady state condition, when the vapor and liquid are at equilibrium corresponding to the membrane surface and the pressure within the membrane pores [1]. The vapour pressure (P^0) within the membrane pores can be determined by the Antoine equation:

$$P^0 = \exp\left[A - \frac{B}{C+T}\right] \quad (1)$$

where P^0 is in Pa and T is the temperature in K. For pure water, the constants A, B, and C are 23.1964, 3816.44, and –46.13, respectively [22]. For non-ideal binary solutions, the

membrane pore vapor pressure can be corrected by taking into account the molar faction of the solute and the solvent (water).

In the DCMD process, heat transfer and mass transfer occur simultaneously. The total heat transferred across the membrane is given by [8]:

$$Q = \left[\frac{1}{h_f} + \frac{1}{h_m + N\Delta H_V / \Delta T_m} + \frac{1}{h_p} \right]^{-1} \times \Delta T_m \quad (2)$$

where h_f, h_m, and h_p are the heat transfer coefficient of the feed, membrane, and permeate, respectively. N and ΔH_V are the molar flux and the heat of vaporisation, respectively. ΔT_m is the temperature difference between the feed and distillate sides of the membrane. The total mass transferred across the membrane can be simply expressed as the product of the mass transfer coefficient and the driving force:

$$N = k_f \Delta P^0 \quad (3)$$

The mass transfer coefficient k_f is a function of the temperature, pressure, and membrane properties. In addition, ΔP^0 can be dependent on the temperature and the actual composition at the membrane surface, which may differ from that of the bulk solution. As a result, the heat flux and the mass flux are interdependent. The coupling mass-heat transfer problem can be solved via numerical iteration. An analytical solution to the mass and heat flux equations can also be obtained based on several simplifying assumptions. In particular, it is assumed that the pressure on each side of the membrane is the same as the saturation of pure water at the temperature at the membrane surface. One can also assume that the heat transfer coefficients on each side of the membrane are equal. This assumption allows for substitution of membrane properties (P^0_m, T_m, and ΔT_m) with their bulk counterparts (P^0, T, and ΔT).

According to Lawson and Lloyd [1, 8], Equation 3 can then be written as a function of the temperature drop across the membrane:

$$N = K\frac{dP^0}{dT}\Delta T = K\frac{P^0\Delta H_V}{RT^2}\Delta T \quad (4)$$

To evaluate the performance of the DCMD system, experiments were conducted with tap water at a distillate temperature of 20 °C and different feed temperatures in the range between 40 °C to 60 °C. The overall mass transfer coefficient can be determined by fitting the flux data to the model (equations 1 and 4) using an optimisation procedure (Solver, Microsoft Excel). Overall, the model and the experimental data are in good agreement (Figure 2). Accordingly, the overall mass transfer coefficient was determined to be 0.0223 (mol/Pa.m^2.s). Because the mass flux is proportional to the temperature gradient across the membrane, permeate flux increased dramatically as the feed temperature increased (Figure 2). It is noteworthy that the performance of the DCMD modelled here is under an ideal condition and with pure water. In a realistic situation when DCMD is used for the treatment of highly saline solutions the membrane surface properties may gradually change overtime making this simplified mathematical model invalid. The process of DCMD of highly saline solutions is further discussed in the next section.

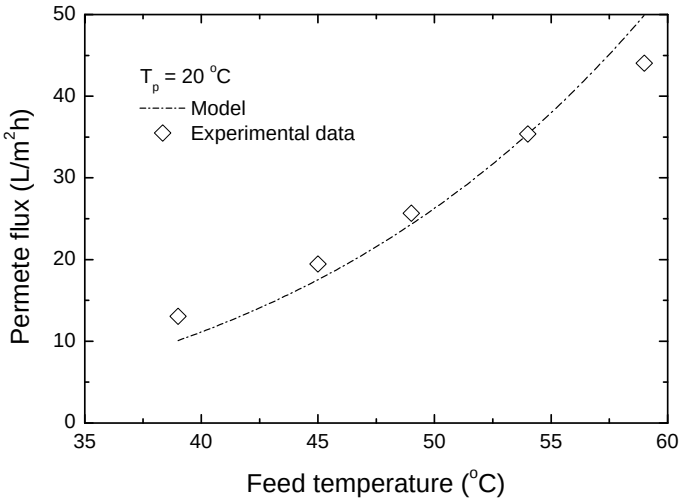

Figure 2: Modelled and experimental permeate flux as a function of feed temperature (Permeate temperature (T_p)=20 °C, V_f=60 L/h, V_p=60 L/h, tap water with pH ~ 7).

3.2. DCMD of saline solutions

The membrane permeate fluxes obtained with the three saline solutions investigated in this study are shown in Figure 3. The initial permeate flux is similar despite the significant difference in composition of the three feed solutions (Table 1 and Figure 3). In fact, this initial permeate flux is also similar to the permeate flux obtained with tap water at the same feed temperature (50 °C). Results reported here reconfirm that up to the salinity of seawater, the influence of the feed solution salinity on the initial permeate flux is negligible [6].

Significant decline of permeate flux was observed with time, potentially suggesting dramatic alteration of membrane surface characteristics due to membrane fouling and/or scaling. The permeate flux during the desalination process of seawater declined slowly over the first 1200 minutes, then sharply dropped to zero over a short period of time. The gradual permeate flux declined could possibly be attributed to the formation of salt crystals on the membrane surface. It is also plausible that the rate of crystallisation would increase as the feed water solution became more concentrated (higher concentration of sparingly soluble salts) and the number of seed crystals had reached the threshold for rapid growth.

During the first 1,200 minutes of DCMD desalination of RO concentration, a notable permeate flux was also observed. The rate of flux decline was higher than that observed with seawater feed solution. The RO concentrate used in this experiment had a high total organic carbon content. In contrast, the organic content in seawater was negligible. Higher flux decline during first phase of DCMD could therefore be attributed to the gradual adsorption of organic foulants onto the membrane surface. Once RO concentrate in the feed reservoir became over saturated, a dramatic flux decline was also observed, similar to that of the desalination process of seawater.

A very different permeate flux profile was observed when the saturated $CaSO_4$ solution was used as the feed. The permeate flux of the saturated $CaSO_4$ solution was stable for

228 approximately 300 minutes, followed by a sudden drop to almost zero. This stable permeate
229 flux could be explained as an induction period for crystallisation of gypsum that has been
230 widely reported in the literature [23-25].

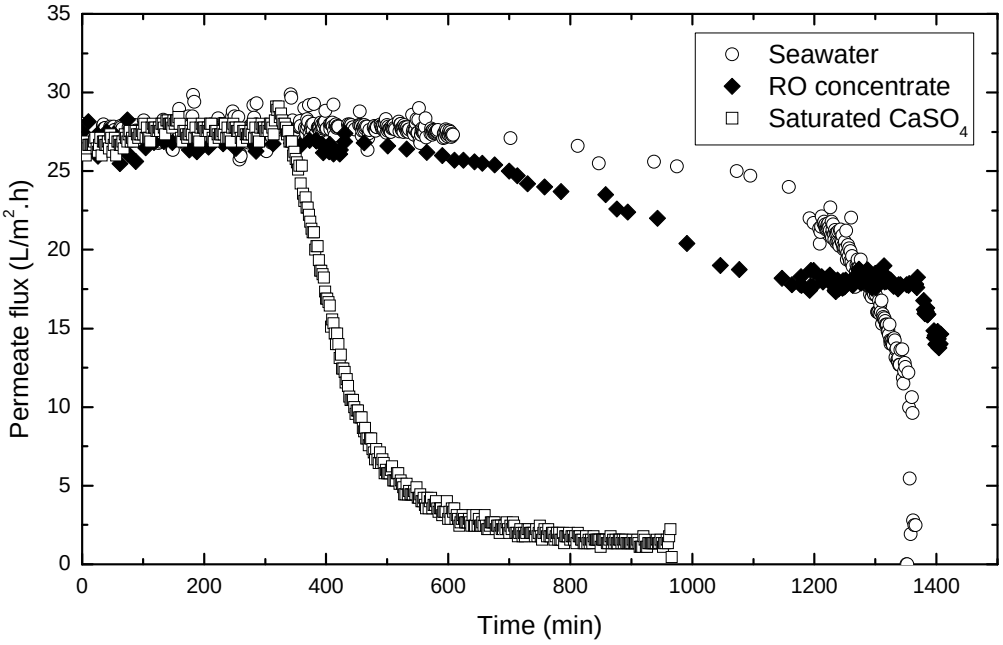

231
232 **Figure 3:** Permeate flux of different saline solutions as a function of time ((Permeate
233 temperature (T_p)=20 °C, V_f=60 L/h, V_p=60 L/h, feed volume = 10 L).

234 SEM micrographs of a virgin membrane side by side with the membrane surfaces after
235 processing the three saline solutions are illustrated in Figure 4. In good agreement with the
236 discussion above, at the completion of the DCMD experiment using seawater, small crystal
237 structures had completely covered the membrane surface (Figure 4B). Similarly, a fluffy
238 amorphous fouling layer can be observed on the membrane surface after the DCMD of RO
239 concentrate (Figure 4C). The formation of the small crystals or the amorphous fouling layer
240 could be attributed to heterogeneous composition of the seawater or RO concentrate
241 solutions. In contrast, the $CaSO_4$ solution used in this investigation had almost no impurities.
242 As a result, large $CaSO_4$ crystals can be seen deposited on the membrane surface at the
243 completion of the DCMD experiment using $CaSO_4$ solution (Figure 4D).

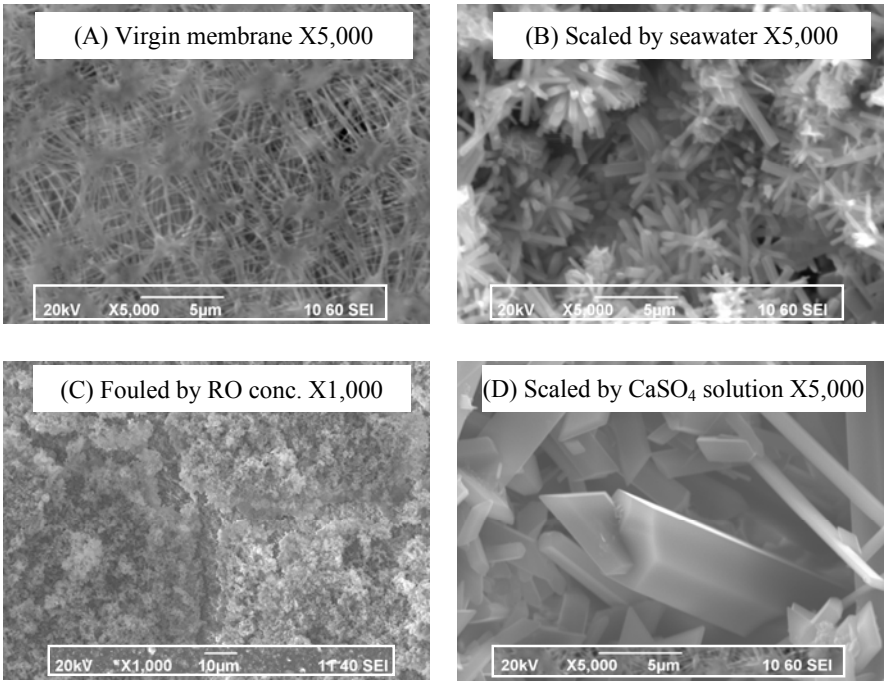

Figure 4: SEM images of the membrane surface under clean and pre-fouled/scaled conditions: (A) virgin membrane, (B) after treating seawater, (C) after treating RO concentrate, and (D) after treating a saturated $CaSO_4$ solution.

The discussion above is consistent with the results obtained from qualitative elementary analysis of the scaling/fouling layers using SEM-EDS. Because the microporous membrane used in this investigation has a PTFE active layer, fluoride and carbon are the only two elements detectable on the membrane surface of a virgin sample (Figure 5A). After the DCMD with each of the three saline solutions, major elements responsible for the scaling/fouling of the membrane surface can be clearly identified in Figures 5B, 5C, and 5D. The presence of calcium is particularly notable in all three cases. In fact, calcium salts are sparingly soluble and calcium is ubiquitous in natural water including seawater and RO concentrate. In addition to calcium, several other metals such as magnesium, aluminium, and molybdenum can also be seen on the membrane surface after processing either seawater or RO concentrate. Once again, it is not surprising that calcium is the only metallic element observed in Figure 5D, which shows the EDS spectrum of the scaling deposit of $CaSO_4$ on the membrane surface.

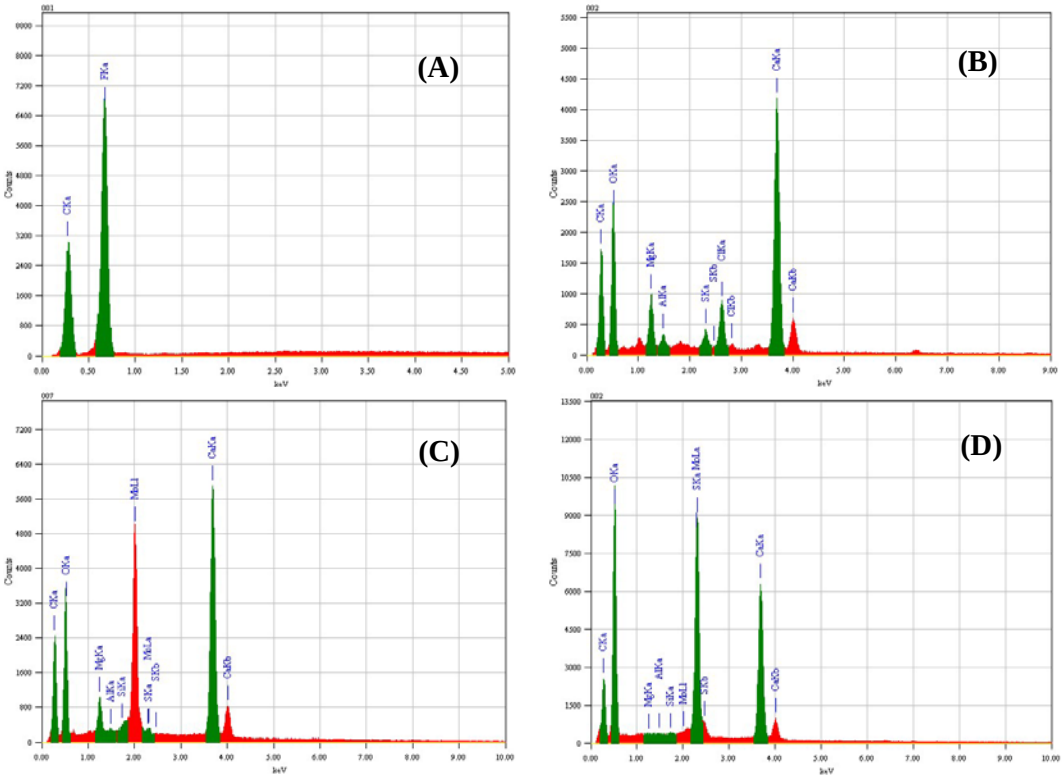

Figure 5: EDS spectra of the membrane surface under clean and pre-fouled/scaled conditions: (A) virgin membrane, (B) after treating seawater, (C) after treating RO concentrate, and (D) after treating a saturated $CaSO_4$ solution.

The deposition of a scaling or fouling layer on the membrane surface does not only restrict the active surface area available for mass transport but also render the membrane surface hydrophilic. The latter can result the wetting of the membrane pores leading to the intrusion of liquid water to the membrane pores, which in turn hinders the mass transfer of water vapour across the membrane. Contact angle measurement conclusively confirms a transformation of the membrane surface characteristic from being hydrophobicity prior to the experiment to very hydrophilic after being used in the DCMD experiment involving any of the three saline solutions (Table 2).

Table 2: Contact angle values of the membrane samples before and after experiments with the three saline solutions.

Sample	Contact angle (^{o})
Virgin membrane	137.7
After treating seawater	8.9
After treating RO concentrate	23.9
After treating saturated $CaSO_4$ solution	8.9

4. Conclusion

Results reported here underscore the importance of membrane scaling and fouling control during DCMD. Scaling and organic fouling were observed with the treatment of seawater and RO concentrate, respectively, resulting in an initial gradual permeate flux decline. In contrast, when the saturated $CaSO_4$ solution was used as the feed, the permeate flux was stable for approximately 300 minutes of operation. However, as the concentration factor of these solutions increased beyond their solubility limit, crystallization of the sparingly soluble salts occurred on the membrane surface, leading to a complete loss of permeate flux at the end of the experiment. Contact angle measurement of the membrane surface revealed a complete loss of hydrophobicity when membrane fouling or scaling occurred. Membrane fouling and scaling were also confirmed by scanning electron microscopy analysis. Results obtained from SEM-EDS analysis of the membrane surface after being used for the desalination of the three saline solutions revealed the ubiquitous presence of calcium in the fouling/scaling layer. Results reported here suggest that pretreatment to remove organic matter and particularly calcium could be essential to prevent membrane fouling and scaling.

5. Reference

[1] K.W. Lawson and D.R. Lloyd, Membrane distillation. J. Membr. Sci., 124(1) (1997): p. 1-25.

[2] F. Macedonio and E. Drioli, Membrane engineering progresses in desalination and water reuse. Membrane Water Treatment, 1(1) (2010): p. 75-81.

[3] A.M. Alklaibi and N. Lior, Membrane-distillation desalination: Status and potential. Desalination, 171(2) (2005): p. 111.

[4] L. Mariah, C.A. Buckley, C.J. Brouckaert, E. Curcio, E. Drioli, D. Jaganyi, and D. Ramjugernath, Membrane distillation of concentrated brines--Role of water activities in the evaluation of driving force. J. Membr. Sci., 280(1-2) (2006): p. 937.

298 [5] C.R. Martinetti, A.E. Childress, and T.Y. Cath, High recovery of concentrated RO
299 brines using forward osmosis and membrane distillation. J. Membr. Sci., 331(1-2) (2009): p.
300 31-39.
301 [6] T.Y. Cath, V.D. Adams, and A.E. Childress, Experimental study of desalination using
302 direct contact membrane distillation: A new approach to flux enhancement. J. Membr. Sci.,
303 228(1) (2004): p. 5-16.
304 [7] V.A. Bui, L.T.T. Vu, and M.H. Nguyen, Simulation and optimisation of direct contact
305 membrane distillation for energy efficiency. Desalination, 259(1-3): p. 29-37.
306 [8] K.W. Lawson and D.R. Lloyd, Membrane distillation. II. Direct contact MD. J.
307 Membr. Sci., 120(1) (1996): p. 123-133.
308 [9] J. Zhang, N. Dow, M. Duke, E. Ostarcevic, J.D. Li, and S. Gray, Identification of
309 material and physical features of membrane distillation membranes for high performance
310 desalination. J. Membr. Sci., 349(1-2): p. 295-303.
311 [10] E. Garcia-Castello, A. Cassano, A. Criscuoli, C. Conidi, and E. Drioli, Recovery and
312 concentration of polyphenols from olive mill wastewaters by integrated membrane system.
313 Water Res., 44(13) (2010): p. 3883-3892.
314 [11] C. Cabassud and D. Wirth, Membrane distillation for water desalination: How to
315 chose an appropriate membrane? Desalination, 157(1-3) (2003): p. 307-314.
316 [12] Á. Kozák, E. Békássy-Molnár, and G. Vatai, Production of black-currant juice
317 concentrate by using membrane distillation. Desalination, 241(1-3) (2009): p. 309-314.
318 [13] G.W. Meindersma, C.M. Guijt, and A.B. de Haan, Desalination and water recycling
319 by air gap membrane distillation. Desalination, 187(1-3) (2006): p. 291-301.
320 [14] J. Phattaranawik, A.G. Fane, A.C.S. Pasquier, and W. Bing, A novel membrane
321 bioreactor based on membrane distillation. Desalination, 223(1-3) (2008): p. 386-395.

[15] M. Gryta, The fermentation process integrated with membrane distillation. Sep. Purif. Technol., 24(1-2) (2001): p. 283-296.

[16] M. Gryta, M. Tomaszewska, and K. Karakulski, Wastewater treatment by membrane distillation. Desalination, 198(1-3) (2006): p. 67-73.

[17] T.Y. Cath, D. Adams, and A.E. Childress, Membrane contactor processes for wastewater reclamation in space II. Combined direct osmosis, osmotic distillation, and membrane distillation for treatment of metabolic wastewater. J. Membr. Sci., 257(1-2) (2005): p. 111-119.

[18] T.Y. Cath, Osmotically and thermally driven membrane processes for enhancement of water recovery in desalination processes. Desal. Wat. Treat., 15(1-3) (2010): p. 279-286.

[19] X. Ji, E. Curcio, S. Al Obaidani, G. Di Profio, E. Fontananova, and E. Drioli, Membrane distillation-crystallization of seawater reverse osmosis brines. Sep. Purif. Technol., 71(1) (2009): p. 76-82.

[20] E. Curcio, X. Ji, G. Di Profio, A.O. Sulaiman, E. Fontananova, and E. Drioli, Membrane distillation operated at high seawater concentration factors: Role of the membrane on CaCO3 scaling in presence of humic acid. J. Membr. Sci., 346(2) (2010): p. 263-269.

[21] F. He, K.K. Sirkar, and J. Gilron, Studies on scaling of membranes in desalination by direct contact membrane distillation: $CaCO_3$ and mixed $CaCO_3/CaSO_4$ systems. Chem. Eng. Sci., 64(8) (2009): p. 1844-1859.

[22] R.C. Reid, J.M. Prausnitz, and T.K. Sherwood, The properties of Gases and Liquids. 3rd ed. 1977, New York: McGraw-Hill.

[23] M. Uchymiak, E. Lyster, J. Glater, and Y. Cohen, Kinetics of gypsum crystal growth on a reverse osmosis membrane. J. Membr. Sci., 314(1-2) (2008): p. 163-172.

[24] D. Hasson, A. Drak, and R. Semiat, Induction times induced in an RO system by antiscalants delaying CaSO4 precipitation. Desalination, 157(1-3) (2003): p. 193-207.

347 [25] D. Hasson, A. Drak, and R. Semiat, Inception of $CaSO_4$ scaling on RO membranes at
348 various water recovery levels. Desalination, 139(1-3) (2001): p. 73-81.